Modifications of the Helbing-Molnár-Farkas-Vicsek Social Force Model for Pedestrian Evolution

Taras I. Lakoba
D. J. Kaup
Institute for Simulation and Training
University of Central Florida, Orlando, FL 32826
dkaup@ist.ucf.edu

Neal M. Finkelstein
Simulation Technology Center
12423 Research Parkway
Orlando, FL 32826

A model of crowd motion that considers each pedestrian as a Newtonian particle subject to both physical and social forces was reported by Helbing, Farkas, and Vicsek in 2000. Subsequent numerical simulations of this model, performed by its authors, showed that it exhibits realistic crowd behavior. In this article, the authors point out that numerical values of certain parameters in that model may produce counterintuitive results when applied to the motion of an *isolated* pedestrian or a *small number* of pedestrians. They have considered modifications of the original model, which allow them to use parameter values that, in the aforementioned sense, are more realistic. However, this is achieved by introducing more features and parameters into the original model. These features are described, and some results of the numerical simulations of the modified model are presented. Two major results of their study need to be mentioned. First, they developed an algorithm, based on an *explicit* numerical integration scheme, which prevents simulated pedestrians from overlapping with one another in physical space. Second, they demonstrated how the form of the social repulsive force between two pedestrians may be deduced from certain measured characteristics of pedestrian flows.

Keywords: Pedestrian dynamics, multiagent simulations, social force models, collective behavior

1. Introduction

1.1 Background

Recently, a considerable amount of research has been done on simulating collective behavior of pedestrians in the street or people finding their way inside a building or a room. Comprehensive reviews of the state of the art can be found [1-5]. Existing models can be broadly separated into the following two categories: (1) discrete-space models and (2) continuous-space ones. Discrete-space, or cellular automata-based, models allow pedestrians to be located at nodes of a fixed or adaptive grid, and pedestrian coordinates are updated at discrete time intervals. Particular models of this category are described in Schadschneider [1]; Blue and Adler [2]; Dijkstra, Jesurun, and Timmermans [3]; Kessel et al. [4]; and Batty, DeSyllas, and Duxbury [5]. The models of the second category allow pedestrians to move continuously in a part of the 2-D surface representing a street, a room, and so forth. The continuous-space models can further be subdivided into the following groups. Some models, such as the ones considered in Helbing [6] and AlGadhi, Mahmassani, and Herman [7], are based on a similarity between the dynamics of a crowd and that of a fluid or gas. Other models of the second category allow pedestrians to choose their paths by optimizing a certain cost function [8]. An interesting model combining the fluid dynamics approach with that of a cost function is considered in Hughes [9]; there the role of the cost function is played by the pedestrian's estimated travel time. Finally, the model considered in other sources [10-12] introduces social and physical forces among pedestrians and then treats each pedestrian as a particle abiding the laws of Newtonian mechanics.

In this report, we focus our attention on the latter model, which we refer to as the Helbing-Molnár-Farkas-Vicsek (HMFV) model. We begin by summarizing the main features of this model, as described in Helbing, Farkas, and Vicsek [11]. In the HMFV model, each pedestrian feels and exerts on others two kinds of forces, "social" and physical. The social forces do not have a physical source; rather, they reflect the intentions of a pedestrian not to collide with other people in the room or with walls and also to move in a specific direction (e.g., toward an exit) at a given speed. When the crowd's density becomes so high that

SIMULATION, Vol. 81, Issue 5, May 2005 339-352

DOI: 10.1177/0037549705052772

pedestrians are forced to collide, the physical forces of pushing and friction enter the picture. Thus, the force exerted on pedestrian i by pedestrian j has the following form:

$$\vec{f}_{ij} = \vec{f}_{\text{social repulsion}} + \vec{f}_{\text{pushing}} + \vec{f}_{\text{friction}} ,$$

where

$$\begin{aligned} \vec{f}_{\text{social repulsion}} &= A\, e^{(R_{ij}-d_{ij})/B}\, \vec{n}_{ij} , \\ \vec{f}_{\text{pushing}} &= k\, \eta(R_{ij}-d_{ij})\, \vec{n}_{ij} , \\ \vec{f}_{\text{friction}} &= \kappa\, |\vec{f}_{\text{pushing}}|\, \vec{t}_{ij} , \end{aligned} \tag{1}$$

Here, A, B, k are constant parameters of the model. In the original study [11], κ was a function of the relative tangential velocity of the two pedestrians; however, in this study, we set it also to a constant. Continuing, $R_{ij} = r_i + r_j$ is the sum of the "radii" of pedestrians i and j; d_{ij} is the distance between their centers; $\vec{n}_{ij}$ and $\vec{t}_{ij}$ are the vectors pointing, respectively, from i to j and in the tangential direction (directed opposite to the velocity of i); and the function $\eta(x)$ is defined by

$$\eta(x) = \begin{cases} x , & x \geq 0 ; \\ 0 , & x < 0 . \end{cases}$$

The first term in equation (1) describes the social force, while the second and third terms describe the physical forces of pushing and sliding friction between the two pedestrian bodies. The form of the function η, multiplying the latter two terms, ensures that they vanish when the pedestrian bodies are not in physical contact. An expression similar to (1) holds for a force between a pedestrian and a wall or another immobile obstacle (e.g., a column) in the room:

$$\vec{f}_{io} = A\, e^{(r_i-d_{io})/B}\, \vec{n}_{io} + k\, \eta(r_i - d_{io})\, \vec{n}_{io} + \kappa\, k\, \eta(r_i - d_{io})\, \vec{t}_{io} . \tag{1'}$$

Here, d_{io} is the distance between the pedestrian's center and the surface of the obstacle (hence o is used for the subindex), and $\vec{n}_{io}$ and $\vec{t}_{io}$ are the vectors normal and tangential to the obstacle's surface at the point where the pedestrian comes in contact with it.

Two additional forces, which arise from the pedestrian's personal considerations, also affect his motion. (Note: Here and below, we refer, for brevity of notations, to the pedestrian as "him" rather than "him or her.") The first force is an attraction force, which makes pedestrians move toward (one of) the exit(s). Following Helbing and Molnár [10], we took this force to have the same functional form as that of $\vec{f}_{\text{social repulsion}}$ (see equation (1)) but with different numerical values of A and B (see Table 1, presented later) and the opposite sign of A, corresponding to attraction rather than repulsion. If there is more than one exit, we assumed that the pedestrian is attracted to the nearest exit that he "sees" (see a discussion about the pedestrian "seeing," or perception, in section 3).

The second of the aforementioned "personal" forces makes pedestrians attempt, at all times, to move at their own preferred velocities. The preferred velocity of a pedestrian is a weighed average between his "own" velocity (having a specified direction) and a "collective" velocity that he perceives around himself. This force has the following form:

$$\vec{f}_{\text{preferred}} = -m\frac{\vec{v}-\vec{v}_0}{\tau}, \quad \vec{v}_0 = (1-p)V_0\vec{e}_i + p\langle\vec{v}_j\rangle_i , \tag{2}$$

where m and $\vec{v}$ are the mass and current velocity of the pedestrian, τ is his "reaction time," $\vec{v}_0$ is the preferred velocity, V_0 is the speed with which the isolated pedestrian would prefer to move, $\vec{e}_i$ is the unit vector along his direction of motion, and $\langle\vec{v}_j\rangle_i$ is the average velocity that the ith person perceives within the radius of 2 to 3 meters around himself. The constant parameter p, referred to in Helbing, Farkas, and Vicsek [11] as a "panic parameter," determines the relative weights of the "own" and "collective" contributions to the preferred velocity. It characterizes how strongly a pedestrian aligns his preferred velocity with the motion of the crowd around him; it might more aptly be called a "co-motion" parameter.

As summarized in Helbing, Farkas, and Vicsek [11], the HMFV model is able to reproduce such phenomena as (1) formation of lanes in both uni- and bidirectional traffic, (2) arc-shaped clogging at an exit when the crowd's desired speed of leaving the room is "too high" (the "faster is slower" effect, explained in detail below) [11, 13], (3) inefficient use of alternative exits when the panic parameter p is either too small or too large, and (4) oscillations of the pedestrian flux at a door through which pedestrians are trying to pass in opposite directions. The reader is referred to a Web site, http://angel.elte.hu/~panic, for an impressive collection of interactive Java applets illustrating the above phenomena. The source code used to obtain the results at this Web site has recently been made available to the public [14]. It is also interesting to point out that a quite different discrete space model, described in Burstedde et al. [15], is also reported to be capable of reproducing the effects of lane formation and periodic oscillations in the pedestrian flux at a door. We emphasize that both the HMFV model and that of Burstedde et al. do not provide pedestrians with any "intelligence" or decision-making capabilities.

1.2 Problems to Be Addressed

In this report, we address two issues concerning the HMFV model and provide solutions to them. The first issue is that the social and physical repulsion forces among pedestrians, defined by equation (1), do not automatically guarantee that any two pedestrians will not overlap during their evolution. By *overlapping*, we mean the following. A pedestrian can be modeled as a circle of radius r_i, which can be squeezed, by the outside pushing forces, to a circle of a smaller radius $r = r_i - s_{\max}$, where $s_{\max}$ is the maximum allowed

magnitude of squeezing. (We take $s_{\max} = 20\%$ of r_i.) Note that the second and third terms on the right-hand side of equations (1) and (1′) are nonzero only for pedestrians who have been squeezed against each other or a wall. However, the forces as given by equation (1) do not limit the depth of this squeezing to $s_{\max}$. That is, during an evolution, based on equation (1), a pedestrian may be squeezed by more than $s_{\max}$. In this case, we say that the pedestrian is "overlapped" (either with another person or with a wall or a column). In other words, overlapping occurs when pedestrians either "walk through each other" or "share the same space."

One way to impose a maximum value on the magnitude of squeezing, and hence eliminate the possibility of pedestrian overlapping in the numerical simulations, would be to take a form of the contact force that creates an impenetrable "potential barrier" between pedestrians i and j. An example of such a force is considered in section 2.1. However, as we explain there, using such a force would cause substantial numerical difficulties in the simulations. Therefore, we need to examine other ways of preventing pedestrian overlapping in the model.

In Helbing, Farkas, and Vicsek [11], where the HMFV model was proposed, the aforementioned overlapping problem was circumvented by choosing a very high value for the elasticity constant, $k = 1.2 \cdot 10^5$ kg/sec^2. This, effectively, turns human bodies into very rigid structures, or very stiff springs, that are resistant to penetration and thereby directly prevent the overlapping among pedestrians. We point out, however, that such a high value of k can result in an unrealistically high contact force: for example, two pedestrians squeezed by 5 cm each would feel the force of 6000 N, or more than seven times their weight (80 kg). Such a large force would likely crush a person. Thus, the first question that we address in this study is the following: can we keep the *form* of the contact force the same as in the HMFV model (and in equation (1)) and, at the same time, eliminate the possibility of pedestrian overlapping using a significantly lower value of k than that used in Helbing, Farkas, and Vicsek [11]?

The second issue of the HMFV model that we address is related to the choice of numerical values of parameters of the social force used in Helbing, Farkas, and Vicsek [11] and at http://angel.elte.hu/∼panic. There, the magnitude A and fall-off length B (see equation (1) of that force were chosen to equal

$$A = 2000 \text{ N}, \quad B = 0.08 \text{ m}. \tag{3}$$

The small value of the fall-off length implies that social forces are substantially different from zero only when two people are on the order of 8 cm apart. We argue that the latter value is unrealistically small. To this end, consider the equations of motion [11] of a single pedestrian moving in a straight line toward a wall:

$$\frac{dx}{dt} = v, \quad \frac{dv}{dt} = -\frac{v - v_0}{\tau} - \frac{A}{m} e^{-|x|/B}, \tag{4}$$

where x is the distance the pedestrian is from the wall. Let us assume that the reaction time of an 80-kg pedestrian is $\tau = 0.5$ sec, and his preferred speed is 1.5 m/sec (5.4 km/h). Solving equations (3) and (4) numerically with the initial conditions $x|_{t=0} \gg B$, $v|_{t=0} = v_0$ produces a plot shown in Figure 1a. The feature to note here is the maximum pedestrian's deceleration: it exceeds the acceleration of gravity, $g = 9.8$ m/sec^2, by almost 40%. This does not appear realistic; see, for example, Figure 12 in Weidmann [16], which suggests that an instantaneous acceleration during normal walking does not exceed 0.2 g. The source of unrealistically high acceleration here is the very small fall-off length, B, rather than a large value of the maximum force, A. To illustrate this point, we show in Figure 1b the result of solving equation (4) with $B = 0.5$ m and the other parameters being the same as above. The maximum deceleration in this case is less than $0.3g$. Moreover, the very small value of $B = 0.08$ m, used in Helbing, Farkas, and Vicsek [11] and at http://angel.elte.hu/∼panic, implies that the social force between pedestrians who are located only 50 cm away is $(2000 \text{ N}) \cdot e^{-0.5/0.08} < 5$ N (i.e., is only on the order of the weight of a baseball). It is clear that such a small force cannot explain why, in a not too dense crowd, the typical distance that people prefer to keep among themselves is on the order of 50 cm. Thus, the second question that we address in this study is the following: will the (possibly modified) HMFV model still produce realistic simulations of crowd motion if the value of B is taken on the order of 0.5 m instead of 0.08 m?

Let us now summarize the motivation and objectives of our work. Our starting point was an observation that the HMFV model made use of "unrealistic" numerical values of certain physical parameters to produce the realistic simulations of crowd motion. We have called these parameter values "unrealistic" because, when they are applied to the motion of a single pedestrian or a pair of pedestrians, they produce counterintuitive results, as explained in detail in the preceding paragraphs. The objective of our work is thus to find a modification of the HMFV model that would satisfy two criteria: (1) it must retain the realism of the HMFV model in crowd motion simulations while, at the same time, (2) it must more realistically describe the behavior of a small number of pedestrians, who are the "building blocks" of a crowd. By a *modification* to the model, we mean both changing the numerical values of its parameters as compared to those reported in Helbing, Farkas, and Vicsek [11] and introducing new features into the model.

In practice, the way we eventually devised these specific modifications was that of a typical genetic algorithm: we introduced a "seed" modification (e.g., took $B = 0.50$ m) and then observed the results of the ensuing simulations. Those results would normally contain some feature(s) that went counter to (our personal experience of) what a realistic crowd behavior should be. Then, we would include further modifications to make that particular feature appear realistic (in the above sense) again. It is, therefore, only

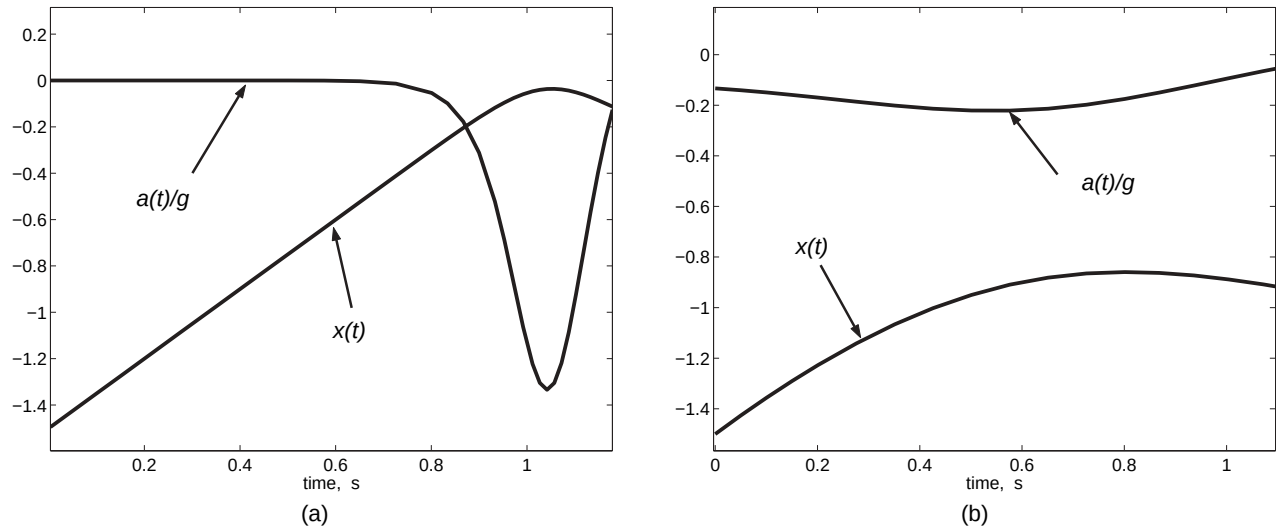

Figure 1. Results of solution of equation (5) with A = 2000 N and B = 0.08 m (a) and 0.5 m (b)

natural that the modifications that we had to introduce are interrelated and thus most likely need to be considered as a single unit.

In a heavy panic situation, one would expect many of the parameters in our modified HMFV model, and perhaps even their functional form, to undergo a dramatic change, wherein the individuals will tend to seek to obtain their own self-survival and may even abandon respect for others. We simply note that at this time, this study does not consider or apply to that situation.

1.3 Outline of the Article

We now give a preview of the results obtained in this study. In section 2, we address the first of the aforementioned issues with the HMFV model: how to prevent overlapping among pedestrians while using a smaller value of the elasticity parameter than the one used in Helbing, Farkas, and Vicsek [11]. First, we demonstrate that equations of motion with a force that creates an impenetrable "potential barrier" between any two pedestrians, thereby automatically guaranteeing the absence of overlapping, cannot be time-efficiently solved by commonly available explicit or implicit integration routines. Then, we describe an original algorithm that we have devised to eliminate overlapping among pedestrians while using the contact forces of the form (1) and a value of parameter k that is substantially smaller than that used in Helbing, Farkas, and Vicsek [11]. We note that our algorithm does not depend on a particular form of the contact force acting on a pedestrian. Therefore, we expect that this method, or some modification of it, would be found useful in other situations dealing with parallel updating of quantities, among which there acts a contact force and some exclusion rules (e.g., as in the case where two pedestrians cannot occupy the same location or two "very close" locations and, as a result, the "stronger" pedestrian pushes the "weaker" one out of that location).

In section 3, we address the second issue with the HMFV model—that is, using a larger value of the fall-off length B of the social repulsive force between any two pedestrians than the value used in Helbing, Farkas, and Vicsek [11]. First, we present an argument that the actual fall-off length must be on the order of 0.5 m. We emphasize that the focus of our discussion is on the *methodology* that allows one to deduce an approximate value of B from certain empirical data, rather than on its precise value per se. Indeed, the aforementioned value of 0.5 m is deduced from data reported in Weidmannn [16] for, apparently, a crowd in a German city. A crowd in another country is likely, due to a different cultural behavior, to exhibit different quantitative characteristics and thus could lead to a different estimate for B.

Once we have established an approximate realistic value for the fall-off length of the social force, we then turn to discussing its maximum magnitude. In doing so, we explain the need for introducing three modifications to the HMFV model: (1) a dependence of the social force on the crowd's density, (2) distinguishing between face-to-back and face-to-face social repulsion forces between any two pedestrians, and (3) allowing a pedestrian to learn and forget the location of the exit(s) and/or obstacles in the room and use this knowledge for selecting his own direction of motion. We emphasize that the above three modifications (and, in fact, complexifications) of the HMFV model were found to be essential to maintain realism of the simulated crowd behavior, which was the remarkable feature of the original model.

Finally, we need to verify results produced by our modified model against some criterion that would indicate whether those results are realistic. Having such a criterion

would allow us to fine-tune the model parameters so as to satisfy it. The criterion we made use of in this study is the "faster is slower" effect [11]. This effect is summarized by the observation that if people in an excited condition are trying to get out of the room too fast, they actually slow down their own egress due to pushing and clogging at the door [13]. In section 4, we present results of numerical simulations, based on the modified HMFV model, for the number of pedestrians exiting a room within a specified time interval. From these results, we find a parameter regime where our modified HMFV model does exhibit the "faster is slower" effect.

Conclusions of our work are presented in section 5.

2. Overlap-Eliminating Algorithm

In this section, we achieve the following two main goals. First, we explain why implementing any model with a physical repulsion force that eliminates overlapping by creating an impenetrable barrier between pedestrians in close contact must always be numerically inefficient. Second, we propose and give a detailed description of a novel and relatively time-efficient algorithm that allows one to implement a crowd model using the repulsive forces of the form (1) (which does not create an impenetrable barrier) and still avoid overlapping among pedestrians, as explained in section 1. To emphasize the visible consequence of this overlapping, we will sometimes refer to it as being "invasive." Along with the details of the algorithm, we explain the procedure of adaptive selection of the time step in our simulations.

2.1 Numerical Stiffness of the Equations of Motion

We begin by explaining the problem that arises when one attempts to numerically solve equations of motion when the contact forces are of the following form:

$$f_{ij,\text{contact}} = C\left[\left(\frac{1}{d_{ij} - R_{ij} + 2s_{\max}}\right)^{\alpha} - \left(\frac{1}{2s_{\max}}\right)^{\alpha}\right], \quad d_{ij} < R_{ij}, \tag{5}$$

and where $f_{ij,\text{contact}} = 0$ for $d_{ij} \geq R_{ij}$. In (5), C and $\alpha \geq 1$ are some constants, and $s_{\max}$ is the maximum allowed magnitude of squeezing, discussed above. Using concepts from elementary mechanics, one can show that any force of this form creates an impenetrable potential barrier between pedestrians i and j and indeed prevents them to come together closer than $R_{ij} - 2s_{\max}$. The aforementioned numerical problem arises because the code has to resolve the motion of a person on two disparate scales. The larger scale is on the order of the size of the room (several meters) since it is motion over those distances that we are mainly interested in. The smaller scale is on the order of a centimeter (or less) because the numerical scheme has to resolve such short distances to guarantee that two pedestrians in contact never invasively overlap. Indeed, the changes in their coordinates are proportional to the force $\Delta x \propto f \cdot \Delta t^2$, and since the contact force (5) grows without bound as the pedestrians move closer to each other, the step size Δt needs to be made increasingly smaller to keep Δx such that the squeezing of each pedestrian would not exceed $s_{\max}$. Otherwise, the simulation enters into an *unstable regime,* meaning that it would falsely produce results showing invasive overlapping, whereas no such overlapping can actually occur for the correct solutions of the underlying equations of motion with a contact force of the form (5)). The problem described here is well known as a problem of numerically stiff equations, described in any textbook on numerical analysis (see, e.g., [17]). It is also well known that explicit numerical integration methods, such as Euler's method, are very time inefficient for stiff problems; the above consideration of Δt is just a particular example illustrating this point. While the computational time required to evolve N pedestrians over one time step grows linearly with N (assuming that a pedestrian feels forces from only those of his fellows who are within a prescribed distance, say, 2 to 3 meters from him), the total computational time is proportional to $N/\Delta t$ and thus becomes very large whenever Δt becomes very small. For example, an early version of our simulator that used expression (5) for the contact forces and a standard explicit ordinary differential equation solver of Matlab took more than 3 hours on a 2.4-GHz Pentium IV machine to compute 60 seconds of evolution of 100 pedestrians exiting a room.

An established alternative to explicit integration methods are implicit methods, which we also explored in an attempt to speed up the computations. For implicit methods, the step size Δt is determined only by the desired accuracy (i.e., $O(\Delta t^n)$, $n = 1, 2, \ldots$) of the computation rather than by any requirement of stability of the numerical scheme (see above). However, the computational time of one step grows as N^2, unless one can exploit the sparse structure of the system of equations of motion, in which case it would be expected to grow as N. (The system of equations in our case is sparse since, as mentioned above, we take into account interactions of a given pedestrian, not with the entire crowd but with only the few people who are found no more than 2 or 3 meters away from him.) We have been unable to find any published record describing an implicit method for a sparse matrix with such a *variable* pattern of nonzero elements. Consequently, we have only been able to test implicit methods by using a standard (i.e., nonsparse) implicit solver of Matlab. For those nonsparse calculations, we found that modeling 60 seconds of evolution of 100 people by using the contact force of the form (5) requires about 1 hour of computational time on a 2.4-GHz Pentium IV. This computational time was rather insensitive to both the preferred speed and the excitement level of pedestrians. (Note that a faster and a more excited crowd produces higher local density because people tend to congregate near particular locations, such as exits.) On the other hand, using our overlap-eliminating algorithm,

described below, along with an *explicit* integration method, we were able to reduce the computational time to between 20 minutes and 1 hour. The lower estimate pertains to a nonpanicking crowd exiting in an orderly manner, while the higher one pertains to a highly excited crowd attempting to flee the room very fast and thus clogging near the door. In the latter case, a large number of overlap eliminations were needed at each time step. Thus, our algorithm yields a clear advantage over the standard (i.e., nonsparse) implicit method when the crowd density is not too high, while for a dense crowd, the efficiencies of our explicit routine and the nonsparse implicit method are similar.

2.2 Description of the Algorithm

We begin a description of the overlap-eliminating algorithm (OEA) by reminding the reader of what we mean by *squeezing* and by *overlapping*. As noted in section 1, a pedestrian can be squeezed when he is being pushed against by others. There is a maximum magnitude of the squeezing, $s_{\max}$. If a pedestrian is squeezed by more than $s_{\max}$, we say that he overlaps, or invasively overlaps, with another person or a wall. The steps of the proposed OEA are as follows.

OEA: Step 1. Find the most overlapped pedestrian. Note that he could be overlapped with walls (and other immovable obstacles in the room, such as columns), other moving pedestrians, and other pedestrians who have been made "stationary" at this time step (see below).

OEA: Step 2. Determine if the found pedestrian is overlapped (but not necessarily most overlapped) with a wall. If he is, move him away from that wall so as to eliminate the overlap and set the component of his velocity, which is normal to the wall, to zero ($v_{n,\,\mathrm{new}} = 0$) while keeping the same value for the tangential component ($v_{t,\,\mathrm{new}} = v_{t,\,\mathrm{old}}$). After moving the pedestrian away from the wall, make him "stationary" and then move other pedestrians away from him so as to eliminate their overlap. The former pedestrian remains "stationary" (i.e., cannot be "unoverlapped" again) until the current round of overlap elimination (OE) is complete. The velocities of the pedestrians who have been moved away from the "stationary" one are set to coincide with the velocity of the latter. (Note that the term *stationary* here does not necessarily imply that the pedestrian in question has zero velocity; it only signifies that this pedestrian is not to be moved until the end of this round of OE.)

If, at the beginning of step 2, it was determined that the pedestrian in question overlaps only with other pedestrians but not with a wall, perform only the step indicated in the second half of the previous paragraph.

OEA: Step 3. Repeat steps 1 and 2 until no overlapping pedestrians are found, but no more times than the number of pedestrians in the room.

Let us note that, strictly speaking, the algorithm described above does not guarantee that it will eliminate overlaps in all conceivable cases. For example, consider a situation where a very dense crowd is formed near a corner of the room and, moreover, the most overlapped pedestrians are not those closest to the corner but those located a few meters away from it. Then these latter pedestrians are made "stationary" first, and those closest to the corner become rounded up by the immovable boundaries from all directions: by the walls forming the corner and by their fellow pedestrians who had already been made "stationary." In such a case, the OEA will not be able to eliminate all of the overlaps. To track down (highly unlikely) situations such as the one just described, we provided in our simulator for making a record of any cases when the OEA is unable to eliminate overlaps. We have not encountered a single such case in the several hundred simulations that we performed. This gives us confidence that the algorithm we propose can be used, in conjunction with an *explicit* integration method, and eliminates overlaps in most realistic situations.

2.3 Size of the Time Step

Proper selection of the time step size in any explicit numerical integration method, to which the OEA belongs, is known to be of paramount importance [17]. Taking the step size to be too small degrades the computational efficiency of the algorithm, while taking it too large can make the numerical results invalid. Below we describe a procedure of selecting the size of the time step that we found to be optimal, in the sense that it yielded reasonable time efficiency for our code, while the simulation results did not change significantly as the step size was reduced further.

Time step selection: Step 1. For each pedestrian, we calculate the minimum distance, $d_{\min}$, between him and the other pedestrians and walls. We then find a *maximum* between $d_{\min}$ and $s_{\max}$: $\widetilde{d}_i = \max(d_{\min}, s_{\max})$. This sets a minimum limit—namely, $s_{\max}$—on the distance $\widetilde{d}_i$ and thus gives the lower bound for the step size Δt from below, as explained in step 2 below.

Time step selection: Step 2. We compute two quantities, $\Delta t_{\mathrm{repulsion},\,i}$ and $\Delta t_{\mathrm{rel.motion},\,i}$, defined for each pedestrian as follows:

$$\Delta t_{\mathrm{repulsion},\,i} = \min_j \sqrt{\frac{\widetilde{d}_i}{\left[\eta(R_{ij} - d_{ij})\, k\, s_{\max} + |f_{\mathrm{social},\,ij}|\right]/m}}\,, \tag{6}$$

$$\Delta t_{\mathrm{rel.motion},\,i} = \min_j \frac{\widetilde{d}_i}{v_{n,\,ij}}\,. \tag{7}$$

Here, $f_{\mathrm{social},\,ij} = A\, e^{(R_{ij} - d_{ij})/B}$ (see equation (1)), and $v_{n,\,ij}$ is the projection of the relative velocity of the ith and jth

pedestrians on the vector connecting their centers of mass. Note that $\Delta t_{\text{repulsion}}$ is a measure of how fast the pedestrians get repelled from each other, and $\Delta t_{\text{rel.motion}}$ determines how fast the pedestrians will move, relative to one another, through the minimal distance $\widetilde{d}$.

Time step selection: Step 3. We take the minimum, $\Delta t_i = \min(\Delta t_{\text{repulsion},\,i},\ \Delta t_{\text{rel.motion},\,i},\ \tau)$; recall that τ is the reaction time of a pedestrian, assumed to be 0.5 sec in Helbing, Farkas, and Vicsek [11] and also in our simulations.

Time step selection: Step 4. Finally, the size of the time step Δt is computed as

$$\Delta t = \beta \min_i \Delta t_i\,, \tag{8}$$

where β is a numerical factor. We chose it so as to guarantee that reducing it further does not change the exit time of a given number of pedestrians, N, by more than X percent. In our simulations, $\beta = 1/8$ was found to be adequate for $N = 100$ and $X = 5$.

We note that OE is a real physical process in that this is what happens as people crowd together. That is, as each person is threatened with overlapping by another, he slightly shifts his position so as to eliminate this threat of overlapping with other people or with the walls. Therefore, there will be some lag time for this physical process of shifting to occur. For each pedestrian, we determine this time as $\Delta t_{\text{OE}} = m(\Delta v)_{\text{OE}}/f_{\text{OE}}$, where $m(\Delta v)_{\text{OE}}$ is the change of the pedestrian's momentum during the act of OE. A new parameter of the model, f_{OE}, is the force applied by the pedestrian's body toward his outside, when he is tightly squeezed. The magnitude of this force is discussed shortly below. Now, considering the actual physical process of OE, the pedestrian in question is assumed to be preoccupied by OE for Δt_{OE} seconds, so that during this time, his coordinates are not updated. If the size of the time step satisfies $\Delta t > \Delta t_{\text{OE}}$, then the modified time step for this pedestrian is $(\Delta t - \Delta t_{\text{OE}})$. If $\Delta t < \Delta t_{\text{OE}}$, then the pedestrian does not evolve over this time step and for $(\Delta t_{\text{OE}} - \Delta t)$ seconds into the next step and so forth, until he is finished with this particular round of OE.

The magnitude of f_{OE} is a free parameter of the model. Ideally, one would like to have as few free parameters in a model as possible, so as to make it easier to calibrate. Note, however, that if one used a model with pushing forces of the form (5) instead of using the OEA, then such a model already has two parameters, C and α, that is, as many as the model that we use here (k and f_{OE}). As far as choosing a numerical value for f_{OE}, we hypothesize that this force is related to the elasticity of the bones of the skeleton, while the pushing force in equation (1) is related to the elasticity of the muscles. Thus, f_{OE} should be larger than $k\,s_{\max}$. We used f_{OE} = 4 mg in our simulations, while $k\,s_{\max}$ = 2 mg. These values appear to be more realistic than the value for the contact force used in Helbing, Farkas, and Vicsek [11] and that we estimated in section 1 to exceed 7 mg.

3. Modifications to the Forces in the HMFV Model

In this section, we address the second of the issues with the HMFV model that was stated in section 1. Namely, we begin by presenting an argument that, for a model to reproduce certain empirical data for a small number of pedestrians, the fall-off length, B, of the social repulsive force should be about 0.5 m, that is, about six times greater than that used in Helbing, Farkas, and Vicsek [11]. However, when we changed the parameter B alone, our simulations produced several unrealistic features of the crowd behavior. For example, we observed that when a pedestrian approached an exit around which there had already been a small group of other pedestrians, then, starting at a certain critical size of that group, the newcomer would turn and run away from the exit, instead of joining those waiting people. By trial and error, we found that for our simulator to produce commonly observed crowd behavior, as the original HMFV model with $B = 0.08$ m does, two modifications to the magnitude of the social force needed to be made. First, we needed to account for a dependence of the social force on the crowd's density. Second, we needed to distinguish between face-to-back and face-to-face social repulsion forces between any two pedestrians. The guideline that we followed in choosing the above modifications was the requirement that our model (1) mimic the commonly observed behavior of an isolated pedestrian or a pair of pedestrians and, of course, (2) produce realistic results for the behavior of a crowd. As a quantitative measure of such realism, we used the exit time of a crowd from a room and showed how this quantity changed with the parameters of the modified social repulsive force. The results allow us to decide in what ranges these parameter values should be chosen. Last, we describe another pair of modifications that we found to add more realism to the model. Namely, we made use of the fact that a pedestrian feels a greater attractive or repulsive social force when he sees an obstacle or an exit than when he is looking in the opposite direction. However, we then had to also include a memory that a pedestrian has of the location of the exit and/or obstacles in the room for the simulated pedestrian to exhibit realistic behavior.

3.1 Fall-Off Length and Functional Form of the Social Repulsion Force

We begin by arguing that the typical fall-off length, B, of the social repulsion force needs to be on the order of 0.5 m to explain the empirical velocity versus density curve for a nonpanicking crowd, reported in Weidmann [16]. This argument consists of several steps. First, the velocity versus density curve has an analytic fit [16]

$$v(\rho) = w_0 \left(1 - \exp\left[-1.91\left(\frac{1}{\rho} - \frac{1}{\rho_{\max}}\right)\right]\right), \tag{9}$$

where w_0 = 1.34 m/sec is the speed of an isolated pedestrian, $v(\rho)$ is the average speed of a pedestrian moving in

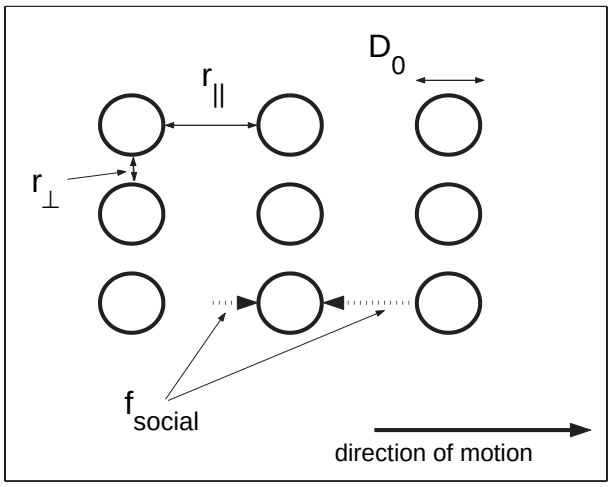

Figure 2. A schematic illustrating motion of pedestrians in lines; see text for details

a crowd in a sufficiently wide walkway, ρ (measured in [ped/m^2]) is the density of the surrounding crowd, and $\rho_{\max}$ is the maximum possible density, reported to be 5.4 ped/m^2 in Weidmann [16]. Next, we need to relate the crowd density with the dimensions of a single pedestrian and typical distances among pedestrians. In our model, we represent each person by a circle of diameter $D_0 \approx 0.7$ m (note that the *minimum* diameter is then $D_0 - 2s_{\max}$). Both Figure 58 in Weidmann [16] and our own simulations suggest that pedestrians in a walkway form (imperfect) lines extending orthogonally to their average direction of motion. This is schematically shown in our Figure 2. Then the density in a moderately dense crowd (say, with $\rho \le 1$ ped/m^2) can be approximated as $\rho = 1/\left[(D_0 + r_\perp)(D_0 + r_{||})\right]$, where $r_{\perp,||}$ are defined in Figure 2. It also follows from simulations (see, e.g., Fig. 3) as well as from the common experience that $r_\perp$ is much less than $r_{||}$ and that it also changes less with the crowd's density. Therefore, for the purpose of this estimate, we take $D_0 + r_\perp = 1$ m.

As the second step in deducing an estimate for B, we consider the following generalization of equations of motion (4):

$$\frac{dx}{dt} = v\,, \tag{10a}$$

$$\frac{dv}{dt} = -\frac{v - v_0(1+E)}{\tau} - \frac{f_{\text{social}}(r_{||})}{m} + b\frac{f_{\text{social}}(r_{||})}{m}\,, \tag{10b}$$

$$\frac{dE}{dt} = -\frac{E}{T} + \frac{E_m}{T}\left(1 - \frac{v}{v_0}\right)\,. \tag{10c}$$

Here, the second term in equation (10b) is the repulsive force that prevents the pedestrian from too closely following the person in front of him, and the third term is the force he feels from the person behind him. (Note the opposite direction of these two forces.) The coefficient b is thus the ratio of the perception by a pedestrian of objects located in front and behind himself [10]. Since a person usually pays less attention to what occurs behind him compared to what occurs in front of him, b must be less than unity. Based on our intuition and a few trial simulations, we took $b = 0.3$ as a reasonable estimate. The actual value of this parameter may depend on the composition of a crowd and, perhaps, other factors. However, choosing a different value for b would only affect the magnitude of the social force (see equation (11) below) but would not invalidate the approach that we follow to obtain that force.

Returning to the parameters introduced in equation (10b), E is the pedestrian's "excitement factor," whose evolution is given by equation (10c). This factor is defined in such a way that its value increases if a pedestrian moves slower than with his preferred speed. Consequently, the effective preferred speed, $v_0(1 + E)$ on the right-hand side of equation (10b), becomes increased, thus reflecting the pedestrian's intention to move faster to "catch up." Note that a similar enhancement factor was used in Helbing, Farkas, and Vicsek [11], where it was defined to instantaneously follow the pedestrian's velocity; in our work, we considered that it would more closely describe reality if this enhancement factor has some "lag time." The first term on the right-hand side of (10c) provides for such a lag time, T. We chose to use $T = 2$ sec as a reasonable value in our simulations. Finally, E_m in equation (10c) determines the maximum magnitude of E; its numerical value is discussed at the end of this subsection.

We now use the equations of motion (10) and the analytic fit (9) to the empirical velocity versus density dependence of a nonpanicking pedestrian flow to deduce an approximate expression for the social repulsion forces acting between any two pedestrians. Assuming a stationarily moving crowd, we set the time derivatives in equations (10) to zero. As long as the crowd is not in a panic state, we also set $v_0 = w_0$ (see (9)) and obtain

$$\frac{f_{\text{social}}(r_{||})}{m} = \frac{w_0\,(1+E_m)\,\exp\left[-1.91\left(D_0 + r_{||} - \frac{1}{\rho_{\max}}\right)\right]}{\tau(1-b)}\,. \tag{11}$$

Not only does this expression confirm the exponential character of the social force, proposed in Helbing and Molnár [10], but it also yields an approximate value for the force's fall-off length in meters: $B \approx 1/1.91 \approx 0.5$. Note that the maximum value of the force cannot be determined from the above considerations because E_m is not yet known. We now turn to discussing this quantity in both nonpanic and panic situations.

In the absence of panic, consider a situation where pedestrian i, walking about 1.5 m in front of pedestrian j, suddenly stops. Common observations suggest that

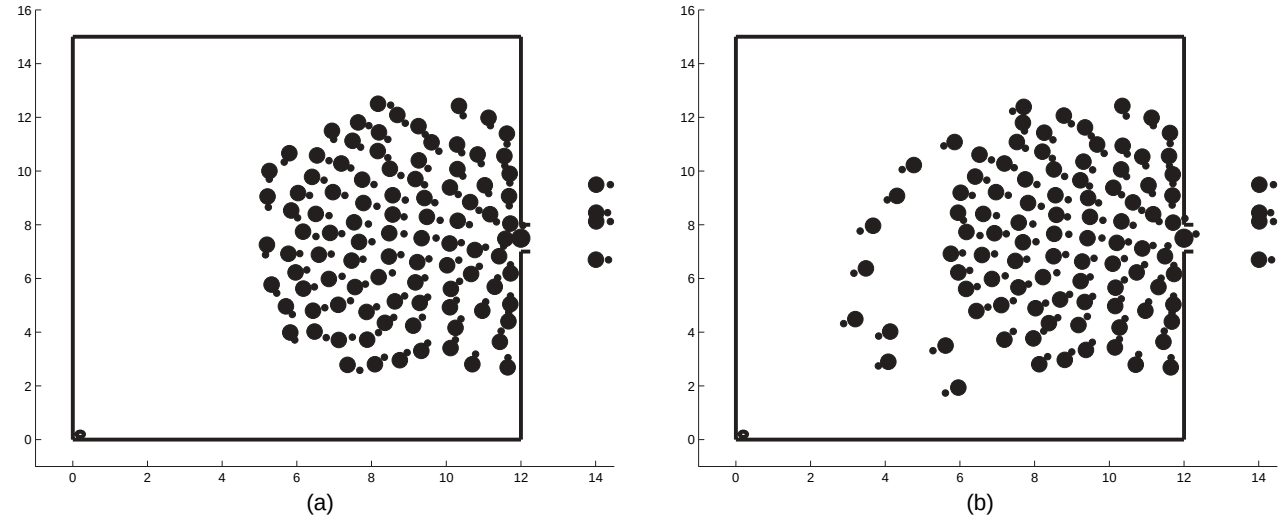

Figure 3. Snapshots of a nonpanicking crowd just before (a) and a few seconds after (b) a group of pedestrians at the back of the crowd "breaks away." Larger circles represent bodies and smaller ones represent noses of pedestrians; in this way, the direction of motion of a pedestrian becomes apparent.

pedestrian j should be able to stop some 30 to 50 cm behind pedestrian i. By numerically solving equations (10) with initial conditions $x|_{t=0} = -r_{||} = -1.5$ m, $v|_{t=0} = v(\rho)$, where $\rho = 1/(D_0 + r_{||})$, and $E|_{t=0} = E_m(1 - v(\rho)/v_0)$, and also using expression (11) for the social force, we find by inspection that the above distance between pedestrians i and j is achieved for $E_m \approx 1$. This is the value that we will use for nonpanicking pedestrians in our simulator.

In the case of a panic situation, the pedestrians will try to hurry rapidly to find an exit. Accordingly, we define a "hurry" parameter by

$$H = v_0/w_0 - 1\,. \tag{12}$$

Recall that $w_0 = 1.34$ m/sec and v_0 are the speed of an isolated nonpanicking pedestrian and the preferred speed parameter, respectively. Once pedestrians are in a "hurrying" state, with v_0 substantially exceeding w_0, then we take the parameter E_m, characterizing the magnitude of pedestrians' excitement above its average level, to be limited and tie this limit to the hurry parameter:

$$E_m = 1/(1 + H)\,. \tag{13}$$

This reflects the fact that the more excited a pedestrian is (and hence the larger value of H he has), the less "room" he has to become even more excited.

Upon inspection of our simulation results, which we display as movies similar to those found at http://angel.elte.hu/∼panic, we found that three modifications to the social force were needed to achieve visible similarities between these movies and common observations of crowd behavior. These modifications are described in the following subsections.

3.2 Density Effects in the Social Repulsion Force

The first of the aforementioned modifications concerns the dependence of the magnitude of the social force on the density of the crowd that surrounds a pedestrian. We observed that if we use the magnitude of f_{social} given by (11), which is independent of the crowd's density, the following two kinds of unrealistic behavior would occur. First, if there occurred a few-seconds delay in the crowd's exiting, pedestrians located at the outer edge of the crowd (i.e., those farthest from the exit) would turn and run away as a group. Figure 3a,b shows snapshots of the crowd just before and a few seconds after this happens in a particular simulation. Second, we also found that it was necessary to use a greater repulsive force than that given by (11) when the crowd is very dense because otherwise, even pedestrians who tend to walk with "normal" speed of 1.5 m/sec would begin to collide and clog the exit.

To correct these behaviors, we found it sufficient to include density effects into the magnitude of the force (11) in the simplest possible (i.e., linear) manner. First, let us separate out the distance dependence on the repulsive social force and reexpress (11) as

$$f_{\text{social}} = f_{\text{social}}^{\max} \exp\left[-1.91 r_{||}\right]\,,$$

where $f_{\text{social}}^{\max}$ is the magnitude of the social force. We now modify this magnitude by multiplying it by the density factor in the last square brackets, see equation (14).

$$\frac{f_{\text{social}}^{\max}}{m} = \frac{w_0\,(1+E_m)\,\exp\left[-1.91\left(D_0 - \frac{1}{\rho_{\max}}\right)\right]}{\tau(1-b)}$$
$$[K_0(1-\widetilde{\rho}) + K_1\widetilde{\rho}]\ . \qquad (14)$$

Here, $\widetilde{\rho} = \rho \cdot \frac{\pi}{4} D_0^2$ is a nondimensional product of the crowd density around a given pedestrian and the pedestrian's area. As such, it gives an "average number" of other pedestrians who can be found inside the area occupied by one person, given the crowd density at a particular location. In all crowds, except the most dense ones, where large groups of pedestrians are squeezed against each other, this normalized density is less than unity: $\widetilde{\rho} < 1$. Continuing with equation (14), the first term in the last square brackets, $K_0(1-\widetilde{\rho})$, is there to gradually suppress the social repulsion as the person approaches a dense crowd. It is only effective for people located at the crowd's edge where they see a relatively low density around themselves. The reasoning for this is that if a nonpanicking person approaches a slowly moving crowd, he needs to become more patient and willing "to wait in line," which corresponds to reducing his tendency to be repelled from others as he approaches the crowd. We have found a value of $K_0 = 0.3$ to work well in correcting this first behavior. The second term, $K_1\widetilde{\rho}$, with $K_1 > 1$, is only substantial for large crowd densities, where it corrects for the second behavior mentioned in the introductory paragraph to this subsection. Results of numerical simulations that helped us to determine the range of the parameter K_1 are presented in section 4 below. In the meantime, we will continue with description of other modifications to the HMFV model.

3.3 Orientational Dependence of the Social Force

The second manner in which we modified expression (11) for the social force follows from the observation that a pedestrian feels stronger repulsion if he faces the face rather than the back of his fellow pedestrian. (Pedestrians encounter each other face-to-face when several of them come almost simultaneously to the same exit.) Note that the considerations leading to equation (11) pertain only to the case of face-to-back interactions because a pedestrian in a file always faces the back and never the face of the person in front of him. Therefore, our argument leading to the estimate $B \approx 0.5$ m is not necessarily valid for the face-to-face social repulsion force. Yet, for the computational convenience, we decided to keep $B = 0.5$ m for this force since we found no observations indicating that it should be otherwise. In analogy with equation (14), we postulate that this force depends on the crowd density in a similar manner:

$$f_{\text{social, face-to-face}}^{\max} = F \cdot (1+E_m)\ [1 \cdot (1-\widetilde{\rho}) + K_2 \cdot \widetilde{\rho}]\ . \qquad (15)$$

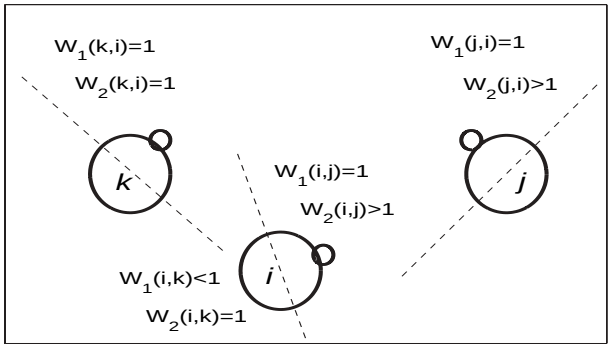

Figure 4. Weight factors multiplying the social repulsive forces acting between pedestrians *i* and *j* and between pedestrians *i* and *k*. Large circles: bodies of pedestrians; small circles: noses of pedestrians, showing the directions where the latter are looking; dashed lines show the boundaries of perception angles of the pedestrians.

Note that the coefficient of $(1-\widetilde{\rho})$ has been absorbed into the overall factor F, which, along with K_2, is a new parameter of the model. Without exploring the possible range of values for K_2 giving realistic behaviors, we have found the value of $K_2 = 1.5$ to work quite well in our simulations, and only this value has been used. Thus, F remains the only parameter of the social force whose range of values remains to be determined. We do this in section 4.

To summarize the results of this subsection so far, we have allowed the magnitude of the social repulsion force to vary between its face-to-back value, given by equation (14), and the larger face-to-face value, given by equation (15). An implementation of this into our code is described next.

To obtain the final expression for the social repulsion force that is exerted on pedestrian i by any other object (i.e., another pedestrian or a wall) in the room, we multiply the face-to-back magnitude (14) by two weight factors, as shown schematically in Figure 4. The first of those, $W_1(i, \text{obj})$, depends on the angle $\phi_{i,\text{obj}}$ between the direction where pedestrian i is looking and the vector extending from him to the object exerting the force:

$$W_1(i,\text{obj}) = \begin{cases} 1, & |\phi_{i,\text{obj}}| < \pi/2 \\ 1-(1-b) & \pi/2 \le |\phi_{i,\text{obj}}| \le \pi \\ \cdot(\phi_{i,\text{obj}} - \pi/2)/(\frac{\pi}{2}), & \end{cases}$$

When the object is a wall, then the angle $\phi_{i,\text{obj}}$ is that between the direction where the pedestrian is looking and the normal vector to the wall. The above form of W_1 guarantees that the pedestrian is repelled less from objects and people who are outside of his perception angle. Also, note that for a pair of pedestrians, i and j, $\phi_{i,j} \neq \phi_{j,i}$ in general.

The second weight factor determines whether we use a face-to-face or face-to-back repulsion force. Clearly, this factor must be different from unity only in the case of social repulsion between two people (but not between a person

and a wall), in which case it is defined by

$$W_2(i,j) = \begin{cases} \dfrac{f^{\max}_{\text{social,face-to-face}}}{f^{\max}_{\text{social,face-to-back}}} > 1, & |\phi_{i,j}| < \pi/2 \quad \text{and} \\ & |\phi_{j,i}| < \pi/2 \\ 1, & \text{otherwise.} \end{cases}$$

Here, the maximum values of the face-to-face and face-to-back forces are given by equations (14) and (15). In other words, this weight factor is different from unity only if both pedestrians are looking in the direction of one another. Note that unlike the first weight factor, for which $W_1(i,j) \neq W_1(j,i)$, the second weight factor is symmetric with respect to interchanging the pedestrians: $W_2(i,j) = W_2(j,i)$—they both have to face each other for the face-to-face interaction to occur.

3.4 Memory Effects

We now describe the third modification to the HMFV model, which we found useful for making the motion of pedestrians look more realistic. Namely, for reasons that are explained shortly below, we found it is desirable to introduce a memory that a pedestrian has about the location of the exit(s). The corresponding memory parameter, M, is governed by the equation

$$\frac{dM}{dt} = -\frac{M}{\tau_\pm} + \frac{\delta M(t)}{\tau_\pm}, \tag{16}$$

where τ_+ and τ_- are the typical times for learning and forgetting about the location of the door, respectively. We chose to use $\tau_+ = 2$ sec and $\tau_- = 10$ sec as reasonable guesses. At each time step, we use either $\delta M(t) = \delta M_+ \equiv 1$ and τ_+, if the door is within the pedestrian's angle of sight ($2 \cdot \pi/2$ rad), or $\delta M(t) = \delta M_- \equiv 0$ and τ_- otherwise. The memory parameter so introduced is always between 0 and 1. The main reason for introducing memory is to define the direction where the pedestrian "looks," which, in turn, determines the vector of his preferred velocity. These quantities are calculated as follows:

$$\vec{e}_i = \left[\frac{\vec{v}_i}{|\vec{v}_i|}(1-\widetilde{\rho}) + \vec{e}_{\text{collective}}\widetilde{\rho} \right](1-M) + \vec{n}_{i,\,\text{door}} M, \tag{17}$$

$$\vec{v}_0 = \vec{e}_i(1+E)V_0(1-p) + \langle \vec{v}_j \rangle_i p, \tag{18}$$

where $\vec{e}_{\text{collective}} = \langle \vec{v}_j \rangle_i / |\langle \vec{v}_j \rangle_i|$ (see equation (2)), and $\vec{n}_{i,\,\text{door}}$ is the unit vector pointing from the ith pedestrian to the door. The term in the square brackets in (17) reflects the tendency of a pedestrian to look in the direction of his own motion when the crowd around him is light and to look in the direction of the crowd's average motion when the crowd is very dense. However, as the pedestrian learns where the door is, he looks mostly in that direction (until, for whatever reason, he forgets about the door). This effect is accounted for by the second term in (17). When that term was absent (which would correspond to pedestrians with no memory), then we observed the counterintuitive behavior by a pedestrian where he begins to change his direction chaotically as he gets into a dense, slowly moving crowd. This occurs because changes to his velocity at every time step become comparable in magnitude with the velocity itself, and thus the sum of the two terms in equation (17) would fluctuate strongly. Introducing the memory factor gives stability to the direction in which the pedestrian seeks to move and thereby eliminates this fluctuation.

4. Simulation Results

Here, we present some results of our numerical simulations of the HMFV model with the modifications described above. In this section, we determine the range of values of K_1 and F in equations (14) and (15) that lead to a realistic crowd behavior. An important criterion of whether a behavior is realistic is whether it exhibits the "faster is slower" effect [11]. Indeed, among the four effects mentioned there, which the HMFV model is able to model, effects (1), (3), and (4), described in section 1, appear to be qualitative rather than quantitative (i.e., they should persist almost irrespective of what parameters for the social force are used). Thus, we concentrate on the ability of our modification of the HMFV model to reproduce the "faster is slower" effect.

To that end, we simulate the evolution of 100 pedestrians in a 12 m × 15 m room with one 1-meter-wide door and record the number of pedestrians who are able to exit the room within 100 seconds. We consider three cases where the values of the pedestrian-preferred velocity, introduced in equation (10b), are $v_0 = 1.5,\ 3$, and 4.5 m/sec. The first case corresponds to pedestrians tending to walk with a "normal" speed, while the last two correspond to pedestrians fleeing the room in different degrees of hurry. Recall that equation (12) related the velocity v_0 to the parameter E_m, defined in equation (10c). Other essential parameters of these simulations (see equations (1), (2)) are as follows: $k = 2.4 \cdot 10^4$ kg/s^2, $\kappa = 1$, $s_{\max} = 7$ cm, $p = 0$ (pedestrians are "independent" of each other), and repulsion of pedestrians from walls is 20% greater than among pedestrians. Moreover, careful modeling of the parameters of the exit door is required to obtain a realistic behavior of pedestrians near that exit [18]. We model the door posts to be 25 cm deep (protruding outside the room) and stiffer than both walls and human bodies, with the corresponding elasticity constant being $k_{\text{ped-door}} = 4.8 \cdot 10^4$ kg/sec^2. The remaining parameters have been specified in the text and are summarized in Table 1. We also add to the forces a small amount (up to 5% of the magnitude of the force) of noise, which serves to help break down possible deadlocks occurring when two pedestrians meet face-to-face at the door.

The number of people exiting the room in 100 sec and having the preferred velocities $v_0 = 1.5$, 3.0, and 4.5 m/sec

Table 1. Parameters of the modified Helbing-Molnár-Farkas-Vicsek (HMFV) model and their values used in our simulations

Symbol	Description	Value Used
A_{exit}	Maximum attraction to an exit	$-mv_0/\tau$ (see below)
b	Back/front pedestrian perception ratio	0.3
B	Fall-off length of social repulsive force	0.5 m
B_{exit}	Fall-off length of attraction to exits	15 m
D_0	Diameter of pedestrian	0.7 m
E_m	Maximum of pedestrian excitement factor	1.0
f_{OE}	Force "unsqueezing" pedestrians in the OAE	Four pedestrian weights
F	Magnitude of face-to-face social repulsive	300-900 N
k	Spring constant	$2.4 \cdot 10^4$ kg/sec^2
K_0	"Willingness to wait" factor for face-to-back orientation	0.3
K_1	High-density correction factor for face-to-back orientation	1.2-2.4
K_2	High-density correction factor for face-to-face orientation	1.5
κ	Coefficient of sliding friction	1
m	Pedestrian mass	80 kg
p	Commotion parameter	0
r_i	Radius of pedestrian	0.35 m
$\rho_{\max}$	Maximum pedestrian density	5.4 ped/m^2
$s_{\max}$	Maximum radial squeezing distance	0.07 m
T	Excitement lag time	2 sec
τ	Pedestrian reaction time	0.5 sec
τ_+	Memory learning time	2 sec
τ_-	Memory forgetting time	10 sec
v_0	Pedestrian's preferred isolated speed	1.5, 3.0, 4.5 m/sec
w_0	Observed isolated pedestrian speed	1.34 m/sec

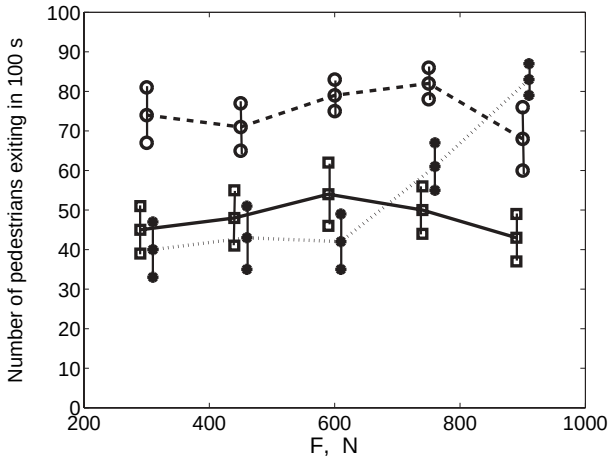

Figure 5. Number of pedestrians who exit a 12 × 15-meter room through a single 1-meter door, plotted as a function of the magnitude of the face-to-face repulsion parameter *F* (see equation (13)). Parameter K_1 = 1.8 (see equation (12)). Other parameters are specified in the text. Squares, open circles, and closed circles correspond, respectively, to preferred pedestrian velocities of v_0 = 1.5, 3, and 4.5 m/sec. The three sets of curves are slightly shifted relative to each other to increase visibility.

is shown in Figure 5 for a fixed value of the parameter $K_1 = 1.8$ (see equation (14)). The free parameter that we vary in this set of simulations is the magnitude of the face-to-face social repulsion force F, defined in equation (15). Each point in Figure 5 represents an average over 25 simulations with randomly selected initial locations and velocities of the pedestrians. Error bars, showing the standard deviations from the mean values, are also plotted. It is clear from these results that our modification of the HMFV model with 300 N $\leq F \leq$ 700 N does indeed show that the "fastest" pedestrians, who prefer to exit at 4.5 m/sec, would actually exit at a much lower rate than the "moderately fast" ones (with $v_0 = 3$ m/sec). In movies that we made from the simulation results, we also observed arc-shaped clogging at the door, which has been reported in previous studies (see http://angel.elte.hu/∼panic).

The next set of simulations (see Fig. 6) shows a dependence of the number of exiting pedestrians on the coefficient K_1 for a fixed value of $F = 600$ N. The "faster is slower" effect is evident here as well for $K_1 \leq 1.8$. However, this effect is violated in the simulations presented in both Figures 5 and 6 when the repulsive force, either face-to-face or face-to-back, is "too high" in a very dense crowd. This is manifested by a dramatic increase in the number of exiting pedestrians with the highest simulated value of the preferred speed, $v_0 = 4.5$ m/sec, when either F or K_1 exceeds certain critical values. This effect may be explained as follows: the stronger the repulsion is among pedestrians, the further away from each other they tend to stay. For the "fastest" pedestrians, who become most densely packed near the exit, the additional distance that they gain by repelling stronger may be sufficient to reduce their squeezing so as to, in turn, reduce the friction and pushing forces that make them clog the door and prevent

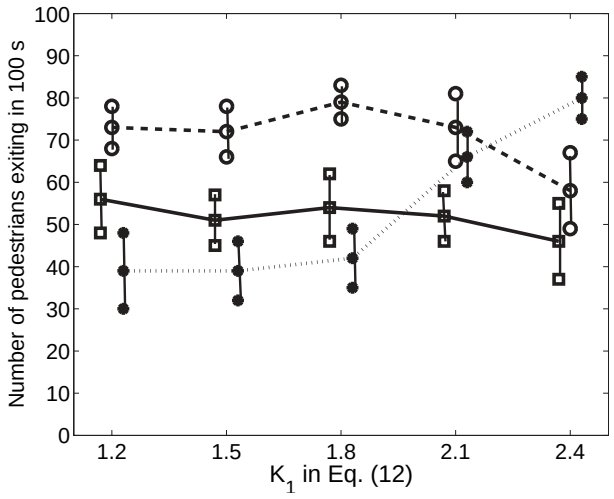

Figure 6. Same as Figure 5, except the number of exiting pedestrians is shown as a function of the parameter K_1 with F = 600 N. Notations are the same as in Figure 5.

exit. It is not clear, however, why the same explanation, at least partially, does not apply to pedestrians who prefer to move at 3 m/sec.

Furthermore, we mention two observations that either go counter to the results of Helbing, Farkas, and Vicsek [11] or that we cannot fully explain based on our intuition. First, in Helbing, Farkas, and Vicsek [11, Fig. 1c], it was pedestrians with $v_0 = 1.5$ m/sec who were found to exit at the highest rate, with the exit rate decreasing with the increase of v_0, while we found that pedestrians with $v_0 = 3$ m/sec exit the room most quickly. The exit times reported in Helbing, Farkas, and Vicsek [11] are also substantially shorter than those deduced from our Figures 5 and 6. Second, Figure 6 suggests that the number of moderately fast pedestrians, with $v_0 = 3$ m/sec, who are able to exit the room *decreases* with the increase of the parameter K_1, while that number increases for the pedestrians with $v_0 = 4.5$ m/sec. The above observations, pointing to differences between simulations of the original HMVF model and our modification of it, call for more observational data on pedestrian egress of a room under various conditions.

5. Conclusions

We have explored a range of numerical values of parameters of the model proposed by Helbing and Molnár [10] and Helbing, Farkas, and Vicsek [11]. We have proposed a number of modifications to the model to produce a more realistic behavior of an isolated pedestrian or a small number of pedestrians while maintaining the realism of the original HMFV model for simulating large crowds.

In section 2, we proposed and implemented a numerical algorithm that allowed one to use an explicit numerical integration scheme for a system of evolution equations and that guaranteed (in most situations) that pedestrians do not overlap. For $N = 100$ pedestrians exiting a room via a single door, this algorithm provided up to a threefold reduction of the computational time compared to a standard implicit numerical solver and an over nine- to over threefold reduction compared to a standard explicit solver with an adaptive step size. Employing this algorithm, we were able to use a realistic value of the contact force that is on the order of two to four human weights, compared to more than seven human weights used in Helbing, Farkas, and Vicsek [11]. We note, however, that in both the original and modified models, the maximum contact force significantly exceeds the weight of a single person. It may be interesting to devise an experiment whereby that force could be measured.

Next, in section 3, we discussed the choice of parameters for the social repulsive force among pedestrians. Moreover, we demonstrated how to obtain the fall-off length of that force from the empirical velocity versus density curve [16] of pedestrian flows in walkways. As explained in section 1, the value of 0.5 m for this parameter appears to be more realistic than the value 0.08 m, used in Helbing, Farkas, and Vicsek [11], as far as the motion of a small number (e.g., two) of pedestrians is concerned. However, this step came at the expense of introducing subsequent modifications to the form of the social repulsive force. These modifications were needed to maintain realism of the simulated behavior of large crowds, as exhibited by the original HMFV model. Specifically, we had to allow the social force to depend on the density of the crowd surrounding a given pedestrian, as well as on whether the pedestrian exerting the force is orientated with his face or back toward the pedestrian on whom the force is exerted. We also found an advantage in assigning to pedestrians a memory of the location of exit(s).

In section 4, we verified that the qualitative results produced by the modified model remained essentially the same as the corresponding results of the original model by presenting numerical results showing how the time in which pedestrians exit a room depends on parameters of the social force. Our results did exhibit the presence of the "faster is slower" effect, originally demonstrated in Helbing, Farkas, and Vicsek [11]. However, the preferred velocity for which the quickest exit time was observed in our simulations was around 3 m/sec—that is, higher than the 1.5 m/sec reported in Helbing, Farkas, and Vicsek [11]. This discrepancy calls both for experimental data on exit times from a room and possibly for further modifications of the HMFV model with moderately long-range repulsion forces. Finding those modifications could be a subject for future research.

We would like to conclude with a few thoughts concerning crowd modeling using the model based on the social force concept. The main strength of the HMFV model, based on the notions of social repulsive forces that keep pedestrians at a distance from each other, is that it does not require any "decision making" by pedestrians. This,

however, may also be a weakness of this model. Namely, in many simulations of exiting pedestrians, we observed that, often, two *nonpanicking* pedestrians would stay face-to-face in front of the door for quite a while (10 seconds and even more) without either of them making a decisive step toward the door and the other pedestrian letting the way. This does not appear to be representative of what actually happens in reality, where similar deadlocks, often caused by "politeness," are normally resolved quicker. Therefore, it seems that the output of the pedestrian model could become even more realistic if some amount of "decision-making" capability were assigned to the pedestrians.

Finally, no matter which specific model is implemented, it will be of limited use until its results can be compared against measured data on pedestrian dynamics. Thus, the greatest need in this field at the moment seems to be to obtain observational data relevant to the existing models.

6. Acknowledgment

We thank D. Helbing and I. Farkas for useful insight on some details of their simulator. We also thank F. Jentsch for help with translating Weidmann's [16] book; P. Kincaid, T. Clarke, B. Goldiez, R. Shumaker, and R. Hofner of the Institute for Simulation and Training for their interest and discussions throughout different stages of this work; and the anonymous reviewers, who made valuable suggestions.

This research has been supported in part by the U.S. Army Research Development and Engineering Command, Simulation Technology Center, contract #N61339-02-C-0107.

7. References

[1] Schadschneider, A. 2002. Cellular automaton approach to pedestrian dynamics—Theory. In *Pedestrian and evacuation dynamics*, edited by M. Schreckenberg and S. Deo Sarma, 75-86. Berlin: Springer-Verlag.

[2] Blue, V. J., and J. L. Adler. 2002. Flow capacities from cellular automata modeling of proportional splits of pedestrians by direction. In *Pedestrian and evacuation dynamics*, edited by M. Schreckenberg and S. Deo Sarma, 115-22. Berlin: Springer-Verlag.

[3] Dijkstra, J., J. Jesurun, and H. Timmermans. 2002. A multi-agent cellular automata model of pedestrian movement. In *Pedestrian and evacuation dynamics*, edited by M. Schreckenberg and S. Deo Sarma, 173-80. Berlin: Springer-Verlag.

[4] Kessel, A., H. Klüpfel, J. Wahle, and M. Schreckenberg. 2002. Microscopic simulation of pedestrian crowd motion. In *Pedestrian and evacuation dynamics*, edited by M. Schreckenberg and S. Deo Sarma, 193-202. Berlin: Springer-Verlag.

[5] Batty, M., J. DeSyllas, and E. Duxbury. 2002. The discrete dynamics of small-scale spatial events: Agent-based models of mobility in carnivals and street parades. Accessed from http://www.casa.ucl.ac.uk/working_papers/Paper56.pdf

[6] Helbing, D. 1992. A fluid-dynamic model for the movement of pedestrians. *Complex Systems* 6:391-415.

[7] AlGadhi, S. A. H., H. S. Mahmassani, and R. Herman. 2002. A speed-concentration relation for bi-directional crowd movements with strong interaction. In *Pedestrian and evacuation dynamics*, edited by M. Schreckenberg and S. Deo Sarma, 3-20. Berlin: Springer-Verlag.

[8] Hoogendoorn, S. P., P. H. L. Bovy, and W. Daamen. 2002. Microscopic pedestrian wayfinding and dynamics modelling. In *Pedestrian and evacuation dynamics*, edited by M. Schreckenberg and S. Deo Sarma, 123-54. Berlin: Springer-Verlag.

[9] Hughes, R. L. 2002. A continuum theory of pedestrian motion. *Transportation Research B* 36:507-35.

[10] Helbing, D., and P. Molnár. 1995. Social force model for pedestrian dynamics. *Physical Review E* 51:4282-7.

[11] Helbing, D., I. Farkas, and T. Vicsek. 2000. Simulating dynamical features of escape panic. *Nature* 407:487-90.

[12] Helbing, D., I. J. Farkas, P. Molnár, and T. Vicsek. 2002. Simulation of pedestrian crowds in normal and evacuation situations. In *Pedestrian and evacuation dynamics*, edited by M. Schreckenberg and S. Deo Sarma, 21-58. Berlin: Springer-Verlag.

[13] Predtechenskii, V. M., and A. I. Milinski. 1978. *Planning for foot traffic flow in buildings*. New Delhi, India: National Bureau of Standards, Amerind Publishing.

[14] Helbing, D., I. Farkas, and T. Vicsek. 2003. Simulation software for "Simulating dynamical features of escape panic." Accessed from http://xxx.lanl.gov, paper cond-mat/0302021

[15] Burstedde, C., K. Klauck, A. Schadschneider, and J. Zittartz. 2001. Simulation of pedestrian dynamics using a two-dimensional cellular automaton. *Physica A* 295:507-25.

[16] Weidmann, U. 1992. *Transporttechnik der Fussgänger*. Zürich: Institut für Verkehrsplanung.

[17] Gerald, C. F., and P. O. Wheatley. 1989. *Applied numerical analysis*. 4th ed. Reading, MA: Addison-Wesley.

[18] Helbing, D., and I. J. Farkas. 2002. Personal communication.

Taras I. Lakoba *is an assistant professor in the Department of Mathematics and Statistics, University of Vermont, Burlington, Vermont.*

D. J. Kaup *holds a Provost Distinguished Research Professorship at the University of Central Florida, Orlanda, Florida, jointly between the Institute for Simulation and Training and the Department of Mathematics.*

Neal M. Finkelstein *is the deputy director of the Simulation and Training Technology Center, University of Central Florida, Orlando, Florida.*